Series-Parallel Connection of Low-Voltage Sources for Integration of Galvanically Isolated Energy Storage Systems

Ramy Georgious, Jorge Garcia, Angel Navarro, Sarah Saeed, Pablo Garcia
LEMUR Research Team, Dept. of Electrical Engineering,
University of Oviedo
Gijon, 33204, Spain
Email: georgiousramy@uniovi.es

***Abstract*—This work explores the Series-Parallel Connection of a Low Voltage Supercapacitor Module to obtain a Hybrid Energy Storage System for grid support applications. The Hybrid System is formed by the Supercapacitor Module itself, intended to ensure fast performance upon peak power requirements, together with a battery that provides the energy requirements. In the full system, the front end converter and the load interfacing converter share a common DC link. The battery is connected to the DC link by means of a Full-Bridge Current-Source bidirectional DC-DC converter. The Supercapacitor Module is connected to the system using a Series-Parallel Configuration, which overcomes the main problems that arise with the most common topologies found in the literature. The full operation of the system has been demonstrated theoretically and by simulations. A demonstration of such connection is shown experimentally, in a converter operating at reduced power levels, in order to validate the feasibility of the system. Conclusions show how this scheme can be used in Hybrid Storage Systems.**

Keywords— Energy Storage Systems, Battery, Supercapacitor, Hybrid Storage Systems, Power Electronic Converters

I. INTRODUCTION

The increasing penetration of distributed generation and Energy Storage Systems (ESS) into the distribution grid is boosting the growth of Microgrids and Smartgrids [1]-[4]. The system under consideration is shown in Fig. 1, in which a Front-End Converter (FEC) connects a given load (which can be generalized as a Microgrid) to the three-phase distribution line. The main ESS, formed by the battery and a Main Storage Converter, is intended to support the DC link voltage in case of load variations or line fluctuations. In this work, the Full-Bridge Current-Source (FBCS) converter, shown in Fig. 2, has been selected as a suitable topology. This main ESS and its associated converter might have limitations in the power rating and bandwidth (due reliability, expected operating life or efficiency constraints). These limitations might affect the transient behavior of the storage system. Upon a power demand from the load, the power will initially be given by the DC link capacitor, which in turn will be discharged. It will take some time, depending on the design, for the ESS to be able to provide the required power to the DC link. This voltage drift might cause problems in the performance of the full system.

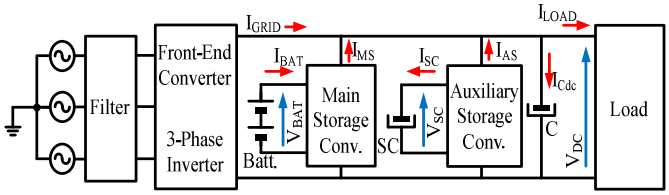

Fig. 1. Block Diagram of the system under consideration (Front-End Converter with ESS).

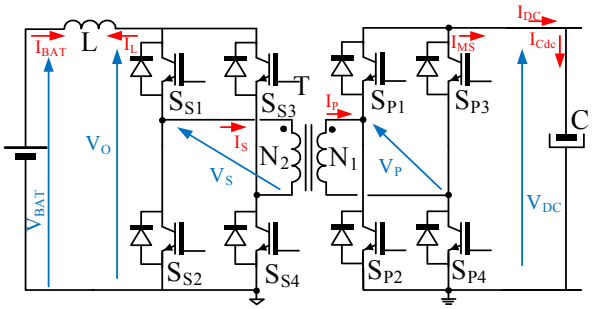

Fig. 2. Full Bridge Current Source (FBCS) converter for interfacing of a DC-link and a battery.

The most current solution is to add in parallel an additional auxiliary storage system, in order to form a Hybrid Energy Storage System (HESS), able to supplement the needed transient power requirements with a very fast dynamics [5]-[11]. This paper is focused on proposing an alternative for this application, based on a Supercapacitor (SC) module, connected to the DC link and the main ESS through a Series Parallel Connection (SPC), shown in Fig. 3 (shaded).

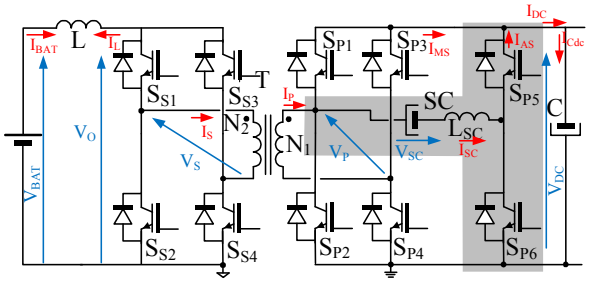

Fig. 3. Full Bridge Current Source (FBCS) converter with SPC connection of Supercapacitor Bank.

II. THE MAIN ENERGY STORAGE SYSTEM

The Main Energy Storage System is connected to the DC link by means of a DC to DC bidirectional Converter. Among the most used isolated topologies, the Double Active Bridge (DAB) converter outstands as a mature, well-known and versatile solution. It provides possibility of soft commutations within some operation margins, and high power density, plus overall good performance. The main flaws of this converter come from the loss of performance at low power levels, and the high current harmonics in the input and output current waveforms [refs required]. In order to avoid such harmonics to flow though the output port (in this case the ESS), in this work, the Current Source version of the DAB has been selected.

The FBCS converter depicted in Fig. 2 is formed by a Full-Bridge structure (switches SP1 to SP4), connected to the primary side of a transformer [12]-[13]. At the secondary side, another Full-Bridge (switches SS1 to SS4) interfaces with a filter inductor, L in series with the battery itself. Unlike in a standard Voltage-Source Double Active Bridge (VSDAB), this inductor operates with high DC current values and relatively small ripples, yielding to a current source behavior in the battery side. This also yields to a more compact design of the inductor, as the AC magnetic field is smaller. This inductor is therefore filtering the current to the battery, thus increasing the system reliability. In addition, the current control through this inductor is also the battery current control, which simplifies the control design.

The switching scheme is depicted in Fig. 4.a, along with the main waveforms of the FBCS converter in steady state. The only control parameter is the duty ratio D that defines the modulation pattern. Fig. 4.b shows simulations of the FBCS operation. Fig. 5.a outlines the control scheme used for the full system. In order to compare the results, the performance of the FEC dynamics has been made equal in both cases (with and without battery). The current reference for the battery is calculated from the actual load step, as shown in Fig. 5.b.

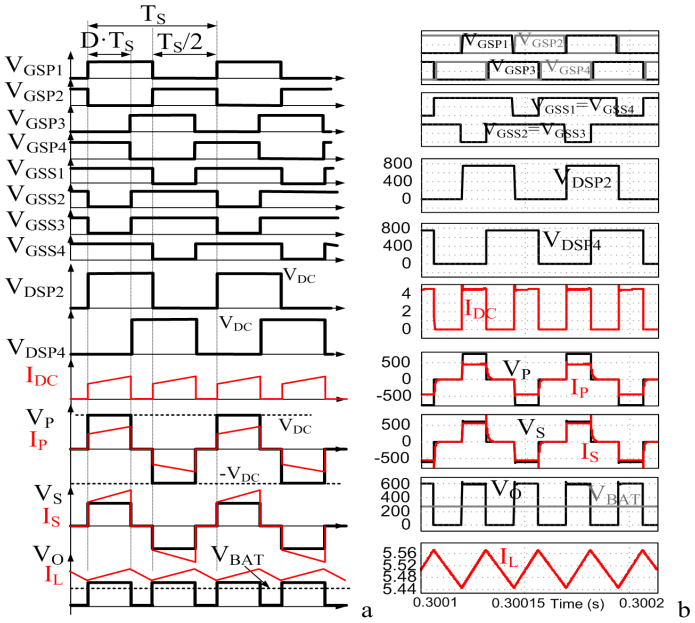

Fig. 4. Main theoretical (a) and simulated (b) waveforms of FBCS operation in steady state

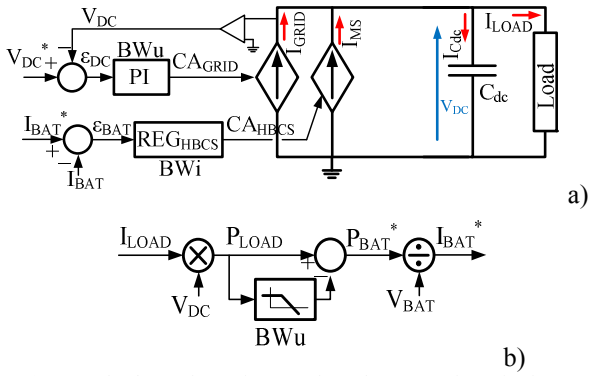

Fig. 5.a) Control scheme for main ESS alone. b) Generation of reference for battery current

Fig. 6 and Fig. 7 depicts the performance of this initial system, without and with the main ESS, for a load step of 1 kW, in a 700 VDC link voltage system. It can be seen how the DC voltage drift is substantially smaller in the system with the main ESS. The rest of the operating parameters are shown in Table I. A closer look to Fig. 7 shows a high di/dt in the initial response after the load step. This might yield to battery operating life shortening, etc. In order to solve this issue, a SC module can be placed in the system, to cope with such transient efforts.

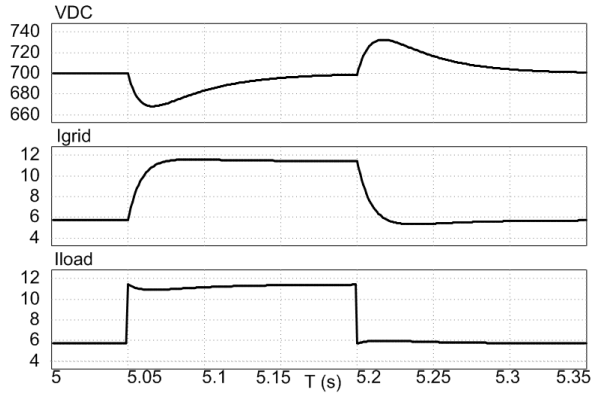

Fig. 6. Simulated waveforms without the main ESS, upon 1kW load step up and down.

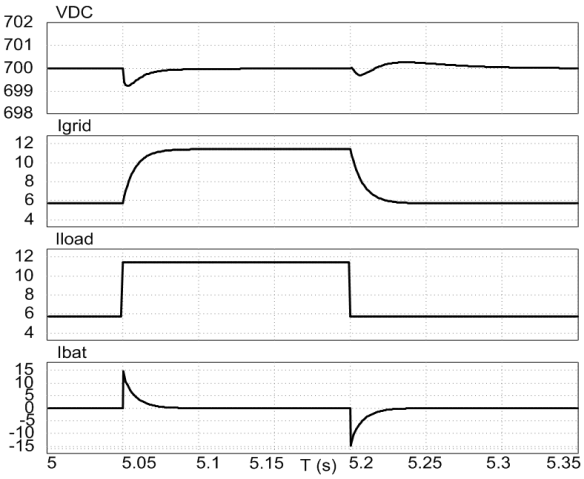

Fig. 7. Simulated waveforms with the main ESS, upon 1kW load step up and down.

TABLE I. PARAMETERS OF THE SIMULATED SYSTEM.

Parameter	Value
DC link ratings	700 VDC
Bandwidth of DC link Control	20 Hz.
Nominal Power (FEC)	10 kW
Battery Nominal Voltage	300 V
Bandwidth of Battery Current Loop	1 kHz.
Load Step	1 kW

III. THE PROPOSED INTEGRATION OF SUPERCAPACITOR

One option for this integration would be the use of a Solid State Transformer (SST), with an additional port for the supercapacitor bank [14]-[15]. This is especially suitable for this application, given the high mismatch voltage ratings among the three ports, which can be solved by selecting the proper turns-ratio of the transformer. However, this would provide high stresses in the transformer, as it must therefore be defined for high currents to avoid saturation during the transients. This work explores the integration of the SC module as an auxiliary leg in the primary side of the converter through SPC, different from the series connection presented in [16], as depicted in Fig. 3.

Ahead is a summary of the principle of operation of the SPC. The simplest connection of the HESS to manage the power flow from and into the storage devices is the Parallel Connection, shown in Fig. 8, based on a dedicated bidirectional boost converter connected to a DC link [17]-[24].

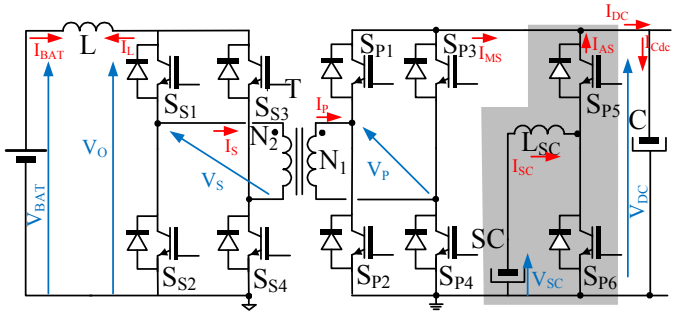

Fig. 8. Full Bridge Current Source (FBCS) converter with direct parallel connection of Supercapacitor Bank.

The main limitations of this connection come from the high voltage mismatch between the supercapacitor voltage ratings and the fixed DC bus voltage. Considering a battery nominal voltage of around half the DC link, then the duty ratio of the battery leg will be around 50%, which optimizes the converter performance, in terms of stresses, design complexity and control capability. However, provided that in some applications the supercapacitor nominal voltage ratings are ranged from 20V to 40V, then for DC bus voltage ratings ranged from 500V to 900V the required gain for the converter might reach values of 40:1 and higher. Such requirements prevent the use of such topology. To overcome this drawback, the Series-Parallel Connection of the supercapacitor modules (Fig. 3) can be carried out. The gain required for the supercapacitor module leg of the converter results in a much more reasonable value than before. Indeed, the drawback of the voltage mismatch at the bidirectional boost configuration is solved, as the average voltage at the midpoint of the supercapacitor module leg results in the addition of the supercapacitors plus the battery voltages. Assuming that the supercapacitor ratings are much smaller than the battery ones, this leg operates with a duty ratio similar to the battery leg. In addition, if the switching pulses are adequately synchronized, the current ripples in the converter might decrease.

Considering steady state, and given that the average voltage at the midpoint of the leg formed by switches S_{P1} and S_{P2} at the primary side equals $V_{DC}/2$, then the average voltage value at the midpoint of the SPC leg (Switches S_{P5} and S_{P6}) will be equal to $(V_{DC}/2)+V_{SC}$, as the average value of the SC inductor voltage is zero. This means that the duty ratio of S_{P5}, D_{SC}, can be calculated as follows:

$$D_{SC} = \frac{V_{SC}+\frac{V_{DC}}{2}}{V_{DC}} \quad (1)$$

Yielding to a value close to 50%, which allows for the operation of this leg with a high gain between the SC module and the DC link, but within the most adequate values for the duty ratio (current and voltage stresses matched, high control margin).

IV. RESULTS AND VALIDATION OF THE PROPOSED SCHEME

Fig. 9 shows theoretical and simulated waveforms of the FBCS converter with the SPC scheme. As it can be seen, the DC current is now the addition of the current given by the main ESS (I_{MS}, from the battery) plus the current given by the Auxiliary ESS (I_{AS}, from the SC module). Fig. 10 shows the control scheme implemented for the control of the converter. As it can be seen, the error of the battery current loop is the parameter that will provide the reference for the supercapacitor current. Fig. 11 shows the performance of the HESS. It can be seen how the main operating parameters are pretty close to the simple battery ones depicted in Fig. 7. However, now the current that the battery is providing has a much slower di/dt, given the peak power is supplied initially by the SC.

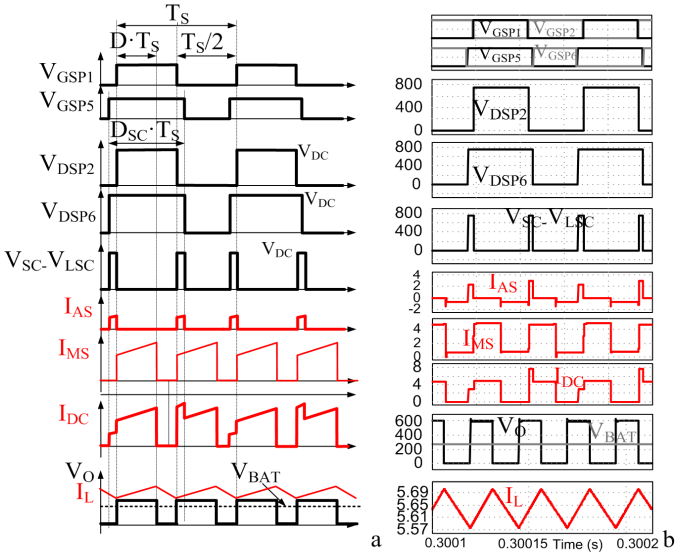

Fig. 9. Main theoretical (a) and simulated (b) waveforms of FBCS operation in steady state with SPC of Supercapacitors.

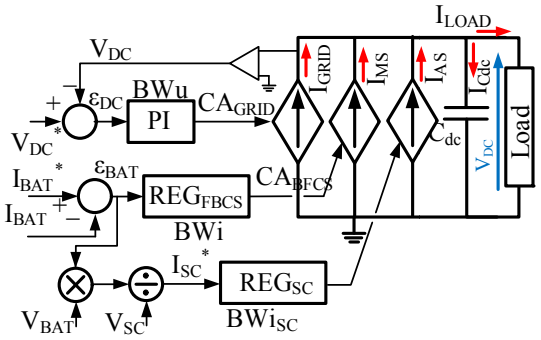

Fig. 10. Control scheme for main and auxiliary ESSs.

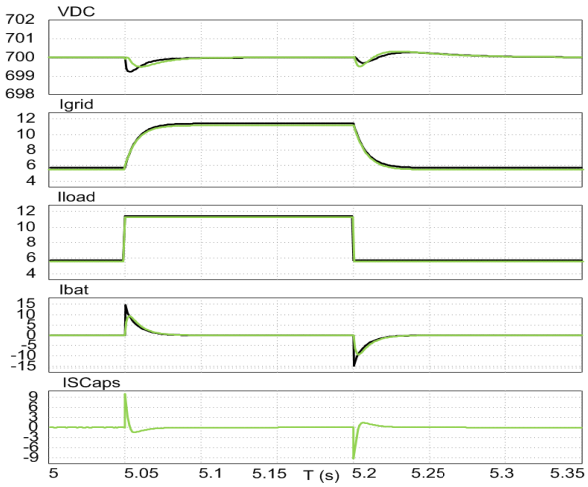

Fig. 11. Simulated waveforms of main ESS alone (black) vs SPC of Supercapacitor, SC, (green), upon 1kW load step up and down.

In order to demonstrate the feasibility of the system, several experimental tests have been carried out in two demonstrator. The first demonstrator consists of a 1kW, 600V_{DC} system, with a supercapacitor bank voltage of 30V_{DC}. Fig. 12 shows the captured data of the SPC scheme operating in steady state. As it can be seen, the leg of the SC (CH7) operates with a duty ratio close to the battery leg (CH6), for 30 V_{DC} and 300 V_{DC} operating voltages, respectively, for a DC link of around 600V.

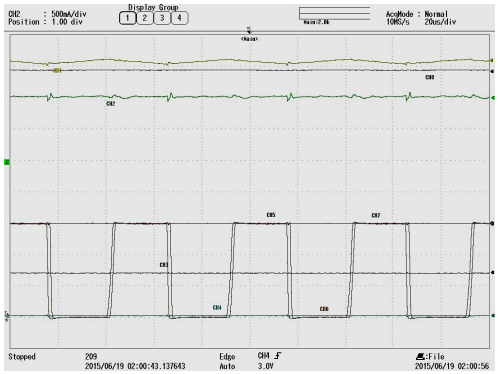

Fig 12. SPC operation of a demonstrator converter. CH1 (yellow): I_{BAT}, 1A/div. CH2 (green): I_{SCaps}, 0.5A/div. CH3 (magenta): V_{BAT}, 200V/div. CH4(cyan): V_{SC}, 50V/div. CH5 (red): V_{DC} , 200V/div, CH6(orange): u_{DSP1}, 200V/div. CH7 (blue): u_{DSP5}, 200V/div. CH8(violet): I_{LOAD},1AV/div. Time: 10us/div

The control system performance has been validated in a scaled prototype, with 200/300V_{DC} in the DC link, around 200V in the battery, 20 kHz switching frequency, and 30 V_{DC} in the supercapacitor bank. The main parameters of the scaled demonstrator are depicted in Table II

TABLE II. PARAMETERS OF THE EXPERIMENTAL SYSTEM.

Parameter	Value
DC link ratings	200/300 V_{DC}
Bandwidth of DC link Control	10 Hz.
Nominal Power (FEC)	1 kW
Battery Nominal Voltage	200 V
Supercaps	20 V
Bandwidth of Supercaps Current Loop	1 kHz.
Load Step	400 W

Fig. 13. shows the performance of a load step in the 300 V_{DC} DC link, and the 10 Hz dynamics of the grid converter. The first trace shows the DC link variation due this load current step (fourth trace), and a voltage ripple of around 10 V can be appreciated.

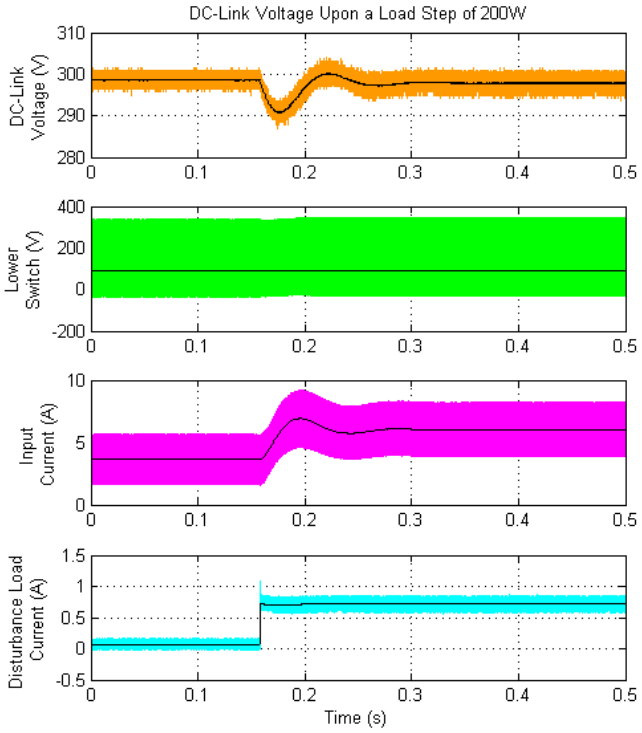

Fig 13. Load step in the DC link, without the supercapacitor module.

Fig. 14. shows the steady state operation of the battery charge, for a 1A charging current reference. The approximately 90º degrees phase shift in the primary side legs of the converter can be seen. Also, the battery current and the battery voltage itself are depicted. The V_{DC} link is in this case equal to 200 V_{DC}.

Fig. 15 shows the operation of the supercapacitor bank under SPC connection, again for 200 V_{DC} link voltage. A current step reference is provided, and the implemented control loop with a bandwidth of 1kHz is shown. As it can be seen, the system is able to track the reference within the desired 1 kHz bandwidth.

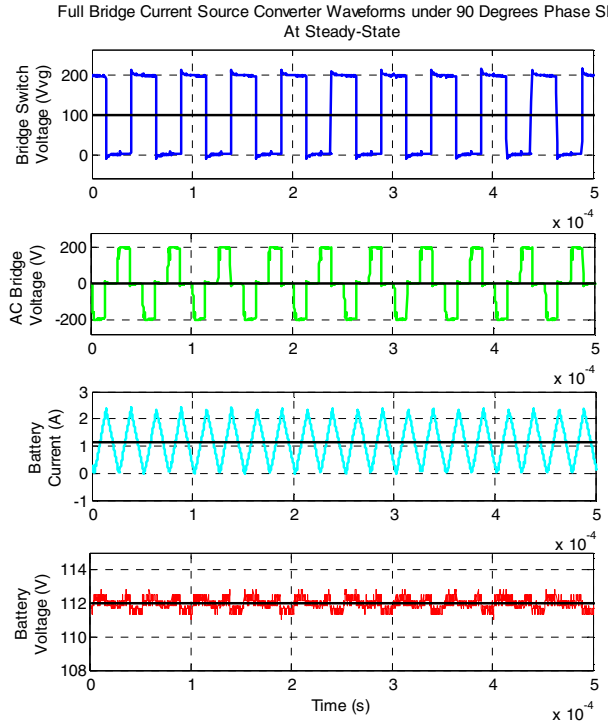

Fig 14. FBCS Converter. Traces (from upper to lower): Voltage in one of the bridge legs (blue); voltage in the primary of the transformer (green); battery current (blue), Battery voltage (red).

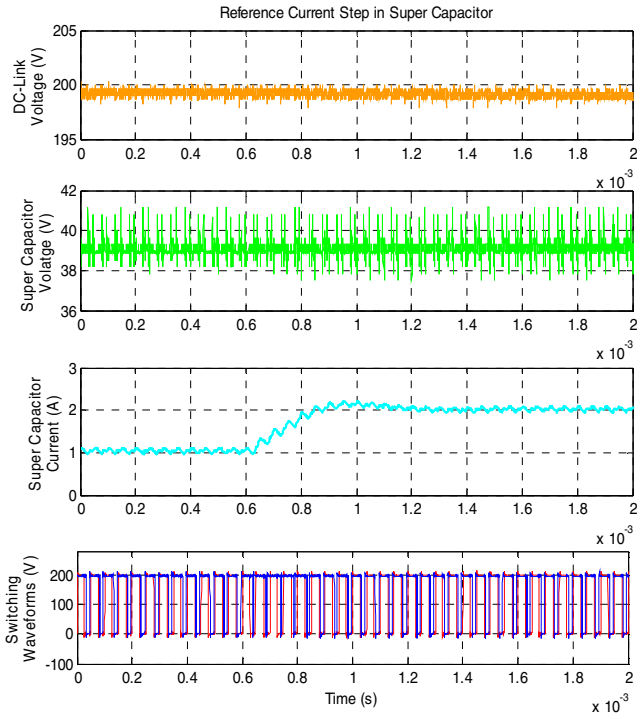

Fig 15. Supercapacitor reference current step. Traces (from upper to lower): DC link voltage (red), Supercaps voltage (green), supercaps current (blue), voltage at both legs of the inverter (lower plot).

V. Conclusion

This work has demonstrated theoretically and through simulations the feasibility of the SPC of a Low Voltage SC Module for interfacing with an ESS formed by a DC link and a Battery connected through the FBCS converter. The main features of this Hybrid System include operation of the system with a high voltage mismatch from the supercaps module to the DC link. It also shows the easy control scheme, design and tuning (fully decoupled control parameters for the main and the auxiliary ESSs). Theoretically this scheme provides higher efficiency than other isolated connections (as the SC energy does not need to flow though the transformer). These characteristics allow this solution to be considered for Hybrid Systems of medium voltage and power ratings.

Acknowledgment

This work has been partially supported by the Spanish Government, Innovation Development and Research Office (MEC), under research grant ENE2013-44245-R, Project "Microholo", and by the European Union through ERFD Structural Funds (FEDER). This work has been partially supported by the government of Principality of Asturias, Foundation for the Promotion in Asturias of Applied Scientific Research and Technology (FICYT), under Severo Ochoa research grant, PA-13-PF-BP13138.

References

[1] P. Thounthong, and S. Rael, "The benefits of hybridization," Industrial Electronics Magazine, IEEE , vol. 3, no. 3, pp. 25-37, Sept. 2009.

[2] A. Hintz, U.R. Prasanna, and K. Rajashekara., "Novel modular Multiple-Input Bidirectional DC-DC Power Converter (MIPC)," In International Power Electronics Conference (IPEC-Hiroshima 2014 - ECCE-ASIA), pp. 2343–50, 18-21 May 2014.

[3] S.D.G. Jayasinghe, and D.M. Vilathgamuwa. "Flying supercapacitors as power smoothing elements in wind generation," IEEE Transactions on Industrial Electronics, vol. 60, no. 7, pp. 2909–18, July 2013.

[4] J. Leuchter, "Review of energy storage for small photovoltaic power source," In Renewable Power Generation Conference (RPG), 3rd, pp. 1–8, 24-25 Sept. 2014.

[5] M. S. Kahn, and M. R. Iravani, "Hybrid control of a grid-interactive wind energy conversion system," IEEE Transactions on Energy Conversion, vol. 23, no. 3, pp. 895-902, Sept. 2008.

[6] I. Vechiu, A. Etxeberria, H. Camblong, and J. M. Vinassa, "Three-level neutral point clamped inverter interface for flow battery/supercapacitor energy storage system used for microgrids," 2nd IEEE PES International Conference and Exhibition on Innovative Smart Grid Technologies (ISGT Europe), pp. 1-6, 5-7 Dec. 2011.

[7] B. Wang, B. Zhang, and Z. Hao, "Control of composite energy storage system in wind and PV hybrid microgrid," IEEE Region 10 Conference (TENCON), pp. 1-5, 22-25 Oct. 2013.

[8] L. Guo, Y. Zhang, and C. S. Wang, "A new battery energy storage system control method based on SOC and variable filter time constant," IEEE PES Innovative Smart Grid Technologies (ISGT), pp. 1-7, 16-20 Jan. 2012.

[9] T. Asao, R. Takahashi, T. Murata, J. Tamura, M. Kubo, A. Kuwayama, and T. Matsumoto, "Smoothing control of wind power generator output by superconducting magnetic energy storage system," International Conference on Electrical Machines and Systems (ICEMS), pp. 302-307, 8-11 Oct. 2007.

[10] X. Han, F. Chen, X. Cui, Y. Li, and X. Li, "A power smoothing control strategy and optimized allocation of battery capacity based on hybrid storage energy technology," Energies, vol. 5, pp. 1593–1612, May 2012.

[11] K. Yoshimoto, T. Nanahara, G. Koshimizu, and Y. Uchida, "New control method for regulating state-of-charge of a battery in hybrid wind power/battery energy storage system," IEEE PES Power Systems Conference and Exposition (PSCE), pp. 1244-1251, 29 Oct. 2006.

[12] D. Maiti, N. Mondal, and S. K. Biswas, "Optimization of a bi-directional hybrid current-fed-voltage-fed converter link," Joint International Conference on Power Electronics, Drives and Energy Systems (PEDES) & 2010 Power India, pp. 1-9, 20-23 Dec. 2010.

[13] P. Xuewei, and A. K. Rathore, "Comparison of bi-directional voltage-fed and current-fed dual active bridge isolated DC/DC converters low voltage high current applications," IEEE 23rd International Symposium on Industrial Electronics (ISIE), pp. 2566–2571, 1-4 June 2014.

[14] Hongfei Wu, Peng Xu, Haibing Hu, Zihu Zhou, and Yan Xing, "Multiport converters based on integration of full-bridge and bidirectional DC-DC topologies for renewable generation systems," IEEE Transactions on Industrial Electronics, vol. 61, no. 2, pp. 856-869, Feb. 2014.

[15] H. Tao, A. Kotsopoulos, J. L. Duarte, and M. A. M. Hendrix, "Family of multiport bidirectional DC-DC converters," IEEE Proceedings Electric Power Applications, vol. 153, no. 3, pp. 451-458, 1 May 2006.

[16] H. Zhou, T. Duong, S. T. Sing, and A. M. Khambadkone, "Interleaved bi-directional dual active bridge DC-DC converter for interfacing ultracapacitor in micro-grid application," IEEE International Symposium on Industrial Electronics (ISIE), pp. 2229–2234, 4-7 July 2010.

[17] W. Li, and G. Joos, "A power electronic interface for a battery supercapacitor hybrid energy storage system for wind applications," IEEE Power Electronics Specialists Conference (PESC), pp. 1762 - 1768, 15-19 June 2008.

[18] H. Yoo, S.-K. Sul, Y. Park, and J. Jeong, "System integration and power-flow management for a series hybrid electric vehicle using supercapacitors and batteries," IEEE Transactions on Industry Applications, vol.44, no.1, pp. 108-114, Jan.-Feb. 2008.

[19] S. D. G. Jayasinghe, D. M. Vilathgamuwa, and U. K. Madawala, "A direct integration scheme for battery-supercapacitor hybrid energy storage systems with the use of grid side inverter," Twenty-Sixth Annual IEEE Applied Power Electronics Conference and Exposition (APEC), pp. 1388-1393, 6-11 March 2011.

[20] Li. Wei, G. Joos, and J. Belanger, "Real-time simulation of a wind turbine generator coupled with a battery supercapacitor energy storage system," IEEE Transactions on Industrial Electronics, vol. 57, no. 4, pp. 1137-1145, April 2010.

[21] N. R. Tummuru, M. K. Mishra, and S. Srinivas, "Dynamic energy management of hybrid energy storage system with high-gain PV converter," IEEE Transactions on Energy Conversion, vol. 30, no. 1, pp. 150-160, March 2015.

[22] S. K. Kollimalla, M. K. Mishra, and L.Narasamma N., "Design and analysis of novel control strategy for battery and supercapacitor storage system," IEEE Transactions on Sustainable Energy, vol. 5, no. 4, pp. 1137-1144, Oct. 2014.

[23] S. K. Kollimalla, M. K. Mishra, and L. Narasamma N., "Coordinated control and energy management of hybrid energy storage system in PV system," International Conference on Computation of Power, Energy, Information and Communication (ICCPEIC), pp. 363-368, 16-17 April 2014.

[24] K. Yamamoto, A. Imakiire, R. Lin, and K. Iimori, "Comparison of configurations of voltage boosters in PWM inverter with voltage boosters with regenerating circuit augmented by electric double-layer capacitor," International Conference on Electrical Machines and Systems (ICEMS), pp. 1-6, 15-18 Nov. 2009.